J Mater Sci (2006) 41:8181–8185
DOI 10.1007/s10853-006-0393-0

Synthesis and electrophoretic deposition of magnetic nickel ferrite nanoparticles

Santosh K. Kurinec · Nkiruka Okeke · Surendra K. Gupta · Heng Zhang · T. Danny Xiao

Received: 3 February 2006 / Accepted: 1 May 2006 / Published online: 28 October 2006

Abstract Powders with particle size ~5–15 nm of nickel ferrite have been synthesized chemically from aqueous precursor solutions. From the structural and magnetic properties, it is determined that the synthetic material possesses high $NiFe_2O_4$ phase purity and controllable particle size. The optimum calcination temperature is found to be ~500 °C, at which the $NiFe_2O_4$ particles exhibit a saturation magnetization of 2800 G, and a particle size of about 10 nm. The particles are then deposited onto silicon substrates by electrophoretic deposition (EPD) process. The Ni ferrite particles are suspended in a medium of isopropyl alcohol with magnesium nitrate and lanthanum nitrate salts as charging agents. The transportation of particles to the substrate surface is assisted by applied electric field and particles adhere to the substrate surface by a glycerol based surfactant. The magnetic response of the EPD film has been investigated by vibrating sample magnetometer (VSM) measurements.

S. K. Kurinec (✉) · N. Okeke · S. K. Gupta
Microelectronic Engineering, Rochester Institute of Technology, 82 Lomb Memorial Drive, Rochester, NY 14623-5604, USA
e-mail: skkemc@rit.edu

H. Zhang · T. D. Xiao
Inframat Corporation, 74 Batterson Park Road, Farmington, CT 06032, USA

H. Zhang
e-mail: hzhang@inframat.com

T. D. Xiao
e-mail: dxiao@inframat.com

Introduction

Trends are emerging for integrating inductive components for the development of miniaturized electronic devices from radar, satellite, telecommunication systems to home radio stereos. Magnetic materials have been a key impediment for the miniaturization of electronic equipment. Consequently, a wide range of novel magnetic materials and process strategies are being explored [1–4]. Conventional inductive components use metallic alloys and ferrites as core materials. The major problem for metallic materials is their low resistivity (~10^{-6} ohm-cm). Since it is impossible to dramatically increase their resistivity, metallic materials were excluded in high frequency applications and ferrites have been the only choice for five decades. Although efforts have been made extensively to improve the performance of the ferrites, very limited progress has been achieved. Recently, a soft solution spin-spray deposition method for nickel ferrite has been reported [5]. Powder synthesis using chemical processes for magnetic materials provides a unique opportunity to modify the magnetic as well as electrical properties of the complex material on a rather large scale [6]. In addition, nanoparticles can be used to form nanocomposites consisting of a magnetic phase and an insulating phase such that the magnetic particles are embedded in the insulating matrix, having essentially no overall electrical conductivity. Nanocomposite processing has provided a new approach for fabricating soft magnetic materials. In a magnetic/ceramic nanocomposite, the resistivity can be drastically increased, leading to significantly reduced eddy current loss. In addition, the exchange coupling between neighboring magnetic nanoparticles

can overcome the anisotropy and demagnetizing effect, resulting in much better soft magnetic properties than conventional bulk materials [7, 8]. After synthesis of nanoparticles, consolidation is a critical step towards application of these materials for device applications. The development of high quality soft magnetic materials with nano size particles will make it possible to miniaturize magnetic devices and integrate them in circuit boards. The study presented here aims to develop a technique for deposition of magnetic films for high frequency device applications.

Electrophoretic deposition (EPD) is a process by which charged particles suspended in a solution are made to migrate by an electric field and are deposited on an electrode. One of the first EP coating applications was in forming an insulating coating of alumina onto tungsten filaments. EPD of powder phosphors, typically 0.5 - 10 μm diameter, is used in the manufacturing of cathode ray tubes (CRT) displays, particularly high-resolution screens [9, 10]. Combination of photolithography and EPD techniques have been employed to fabricate color phosphor screens [11]. Recently, EPD coating of Mn–Zn ferrites in conjunction with electrolytic plating and chemical mechanical planarization (CMP) of copper has been employed in the fabrication of on-chip inductors [12, 13]. However, for high frequency (~GHz) applications, Ni ferrite is desired due to its superior magnetic properties at high frequencies.

Experimental

Nano powder synthesis

A low temperature approach based on the aqueous synthesis method has been developed to synthesize very fine $NiFe_2O_4$ particles. The procedures include (1) preparation of a salt solution that contains Ni and Fe with the selected atomic ratio, (2) addition of the NH_4OH solution into the Ni and Fe precursor solution to adjust pH, without any precipitation, (3) conversion of the precursor solution into a Ni–Fe–O complex powder, and (4), conversion (calcination) of the Ni–Fe–O material into nano size $NiFe_2O_4$ at low temperature in oxygen controlled atmosphere.

Deposition of nanoparticles

The electrophoretic deposition process used in this study was similar to the previously reported process for oxide phosphors and Mn–Zn ferrite [10, 12]. The solution consisted of isopropyl alcohol (IPA) (4g/L) with dissolved nitrates salts (10^{-3} M $Mg(NO_3)_2$ and 10^{-3} $La(NO_3)_3$). Glycerin (1 vol%) was added to the solution bath to disperse particles and as a surfactant to promote increased substrate adhesion. The dissociation of nitrates in the solution bath provides ions to charge the ferrite particles. The ferrite particles, nitrates and 200 mL of IPA were well mixed and agitated with glass beads and then added to the remaining IPA and glycerin solution just prior to plating. An electric field of ~100 V/cm was applied with negative terminal connected to the wafer to be plated and aluminum electrode is used as the anode. The substrate was made conducting where the coating is desired. The anode and cathode were 2 cm apart and placed vertically in the plating bath container. The deposition occured primarily during the first 5–10 min after which current density decays. The current density during the deposition ranged from 0.20 mA/cm^2 to 0.25 mA/cm^2. The films were examined under a scanning electron microscope (LEO EVO 50) and atomic force microscope (Asylum MFP-3D) for morphology. Magnetic properties were investigated using a vibrating sample magnetometer (VSM DMS 1660).

Results and discussion

Powder synthesis

Synthesized powders were calcined at 100, 300, 500, 700, 900 and 1100 °C in an oxygen controlled atmosphere. A sample from each calcination was characterized by X-ray diffraction (XRD) using a Bruker D-5005 diffractometer with Cu K_α radiation to determine the crystal structure and particle size. XRD patterns were obtained using step scanning

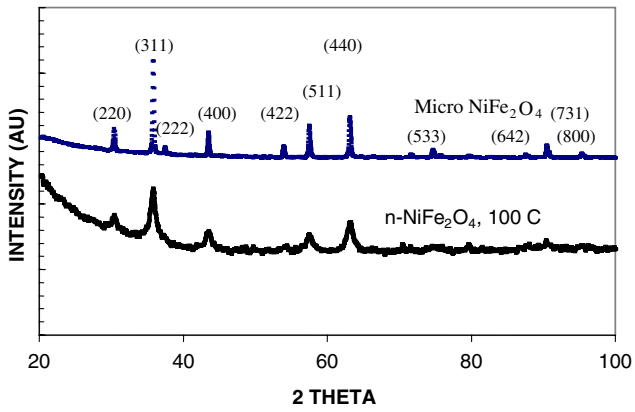

Fig. 1 XRD pattern for nanoparticles of $NiFe_2O_4$ (n-$NiFe_2O_4$) and microsized (bulk) $NiFe_2O_4$

with a step size of 0.02° in 2θ-range of 20° to 100° and counting time of 1 second at each step. Figure 1 shows the XRD patterns of a conventional micrometer sized $NiFe_2O_4$ powder sample as well as the sample calcined at 100 °C. In Fig. 1, XRD peaks are labeled using PDF#54-0964 from the ICDD PDF-4 relational database, and indicate that both samples have inverse spinel crystal structure. Diffraction peaks for the nanometer sized nickel ferrite (n–$NiFe_2O_4$) sample are significantly broader than those for the micrometer sized sample indicating a very small particle size. Samples calcined at higher temperatures show similar XRD patterns. Thus, the designed synthesis approach used is valid. Mean particle size "D" in each sample was determined using peak width at half maxima (WHM) of the 311 peak ($2\theta \sim 35.7°$) and the Scherrer relation [14] given in Eq. (1) below:

$$D = \frac{0.89\lambda}{\sqrt{W^2 - W_0^2}\cos\theta} \quad (1)$$

where λ is the Cu-K_α wavelength, θ is the diffraction angle at the peak maxima, W and W_0 are the WHM from the nano sized and micrometer sized $NiFe_2O_4$ samples, respectively. No particle size related peak broadening is expected for the micrometer sized $NiFe_2O_4$ sample.

Figure 2 shows the mean particle size of the synthesized $NiFe_2O_4$ nanopowders as a function of the calcination temperature. The plot shows that when calcination temperature is ≤500 °C, the mean particle size is small, ~10 nm and constant. For calcination temperatures ≥700 °C, the mean particle size increases significantly with increasing calcination temperature.

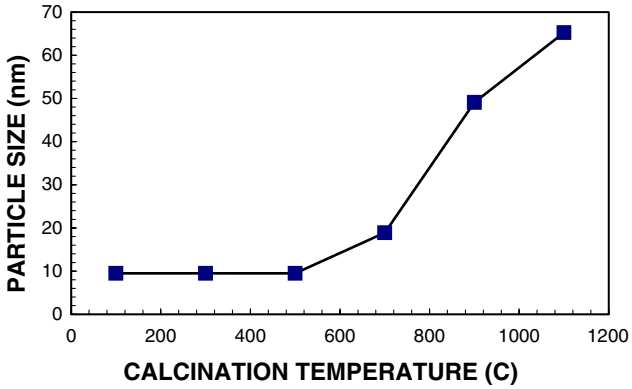

Fig. 2 The particle size of n-$NiFe_2O_4$ as a function of the calcination temperature

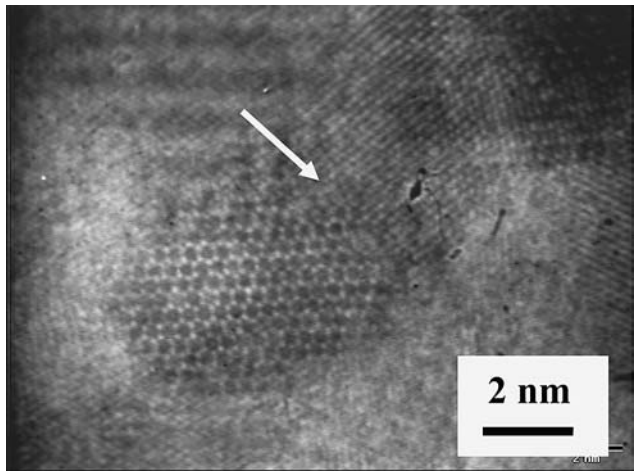

Fig. 3 TEM micrograph showing the microstructure of the Ni-ferrite particles calcined at 500 °C. The arrow points to the boundary between two nanoparticles

For high resolution transmission electron microscope (HRTEM) analysis, specimens were prepared by dispersing the powders in methanol. Drops of this solution were then deposited on a carbon-grid and bright field images, electron diffraction, and lattice images were obtained. A typical HRTEM atomic resolution image shows the morphologies of the ferrite nanoparticle materials in Fig. 3. TEM studies at atomic resolution and electron diffraction reveal that the synthetic $NiFe_2O_4$ nanoparticle is cubic. The size range of the ferrite particles is ~5–15 nm.

Static magnetic properties of a magnetic material are characterized by its magnetization curve, hysteresis loop and the magnetization versus temperature curve. In the characterization of the synthetic $NiFe_2O_4$ nanoparticle, a Quantum Design SQUID magnetometer is used. The measurement temperatures were set to vary between 10°K and 400°K. Figure 4 shows the saturation magnetization as a function of calcination

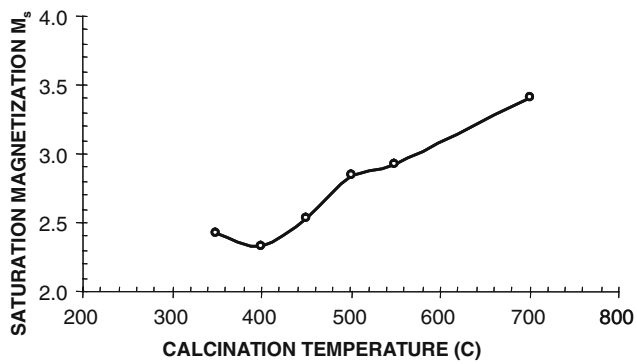

Fig. 4 The variation of saturation magnetization with calcination temperature for $NiFe_2O_4$ powders measured at 10 K

temperature. Calcination at elevated temperatures >400 °C makes the $NiFe_2O_4$ phase more complete thus increasing the magnetization. For conventional microsized $NiFe_2O_4$, its saturation magnetization is 3500 G. As shown in Fig. 4, the same value can be reached for the synthesized nanosized $NiFe_2O_4$ when calcined at 700 °C.

Based on the structural and magnetic properties, it is determined that the synthetic $NiFe_2O_4$ particles possess high phase purity and controllable particle size. The optimum calcination temperature is about 500 °C, at which the $NiFe_2O_4$ nanoparticle possesses a saturation magnetization of 2800 G, and an average particle size of about 10 nm.

Electrophoretic deposition

The EPD process resulted in a self limiting deposition process. Figure 5 shows scanning electron micrographs showing the morphology of the deposit. A film with an average thickness of 2.5 μm is obtained in the first 5 min of deposition. Figure 6 shows the magnetization curve of the EDP film of Ni ferrite particles obtained using a vibrating sample magnetometer. As deposited films exhibit magnetic response that is consistent with the soft behavior of Ni ferrite. The magnetization values depend on the packing density. An isolated nanocomposite particle possesses very high anisotropy due to its large surface anisotropy and demagnetizing effect. For nanocomposite materials, the soft magnetic properties originate from the intergrain interaction, mostly due to the exchange coupling of the neighboring magnetic nanoparticles. The intergrain interaction tends to average the anisotropy of each individual particle, resulting in much reduced anisotropy and, consequently, higher permeability. A critical parameter, the exchange coupling length, is the distance within which the magnetic moments of the two particles can be coupled. For Co and Fe, the exchange length is estimated to be ~35 nm. Examining the film using an atomic force microscope does reveal regions with non-uniformities as shown in Fig 7. Some of these non-uniformities are caused by the post deposition drying process and further optimization needs to be done to get uniform depositions at nanoscales. The EPD process offers an advantage for directed assembly of nanoparticles, a process that is compatible with standard semiconductor processing.

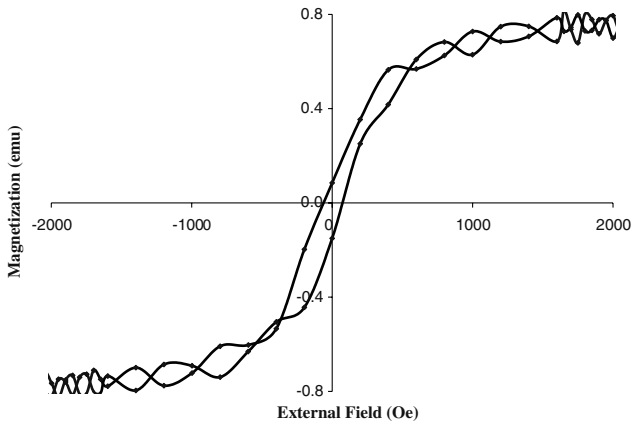

Fig. 6 Magnetization characteristics of electrophoretically deposited film of $NiFe_2O_4$ nanoparticles obtained using a vibrating sample magnetometer

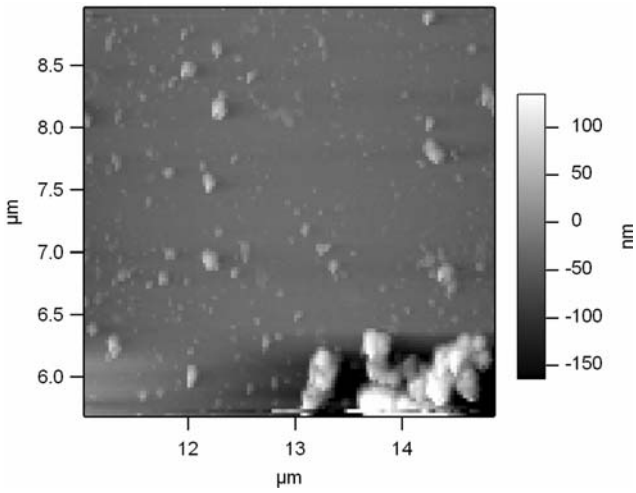

Fig. 7 Atomic force micrograph of electrophoretically deposited film showing nanoscale regions of non-uniform deposition

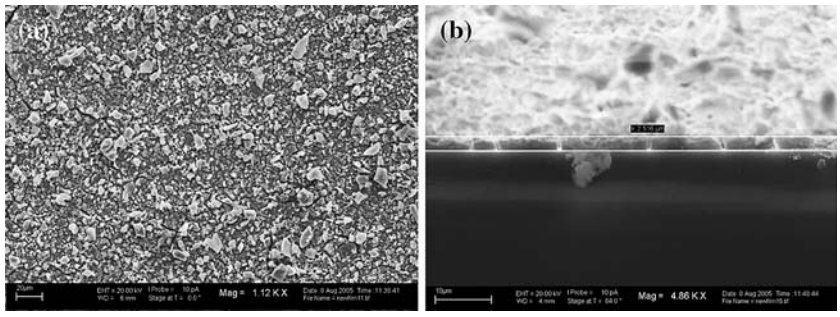

Fig. 5 Scanning electron micrograph of electrophoretically deposited $NiFe_2O_4$ (a) top view; (b) cross-sectional view

Conclusions

An aqueous low temperature process to synthesize $NiFe_2O_4$ particles is developed. Synthesized NiFe2O4 particles have an inverse spinel crystal structure. For calcinations temperatures ≤500 °C, the mean particle size is essentially constant at ~10 nm. For calcinations temperatures >700 °C, the mean particle size increases with increasing calcinations temperature. Electrophoretic deposition of Ni ferrite nano particles prepared by this method has been demonstrated using an isopropyl alcohol based solution containing charging agents.

Acknowledgements This work was supported in part by the National Science Foundation under the Grant Number ECS-021937. The authors are grateful to the US Air Force support under an SBIR Phase II Contract F29601-02-C-0031. The authors thank Dr. Y.D. Zhang of Inframat Corporation for performing the magnetic measurements of the as-synthesized powders.

References

1. Yamaguchi M (2001) IEEE Trans Microwave Theory Techniques 49(12):2331, December
2. Sim S (2002) IEEE Electron Device Lett, 23(12):740, December
3. Korenivski V (2000) J Magnetism Magnetic Mater 215–216:800
4. Ahn CH, Allen MG (1998) IEEE Trans Magnetic, 34(4):866, July
5. Caruntu G, Dumitru I, Bush GG, Caruntu D, O'Connor CJ (2005) J Phys D: Appl Phys 38:811
6. Zhang YD, Wang SH, and Xiao TD (2004) Insulator coated magnetic nanoparticulate composites with reduced core loss and method of manufacture thereof. US Patent No. 6,720,074 B2 (April 13)
7. Ma XQ, Zhang YD, Ge S, Zhang ZT, Yan D, and Xiao TD (2004) Thick film magnetic nanocomposite films and method of manufacture thereof. US Patent Appl. May, Publ. No. 2005/0074600 A1
8. Ge S, Ma XQ, Zhang ZT, Wu MZ, Zhang H, Zhang YD, Ings J, Yacaman MJ (2003) J Appl Phys 93(10):7498
9. Sasaki KY, Talbot JB (1999) Adv Mat 11(2):91
10. Talbot J, Sluzky E, Kurinec SK (2004) J Mater Sci 39(3):771
11. Kurinec SK, Sluzky E (1996) J Soc Information Displays 4(4):371
12. Washburn C, Brown D, Cabacungan J, Venkataraman J, Kurinec SK (2005) Materials Research Society symposium proceedings. Materials, integration and technology for monolithic instruments, 869:157
13. Washburn C, Jorne J, Kurinec S (2006) Electrophoretic deposition: fundamentals and applications II. In: Boccaccini AR, Van der Biest O, Clasen R (ed) Proc. 2nd int. conf. on electrophoretic deposition, Barga, Italy May 29–June 2, 2005. Trans Tech Publications, Key Eng. Mater. 314:127
14. Jenkins R, Snyder RL (1996) Introduction to X-ray powder diffractometry, John Wiley & Sons, New York, p 90